Electronic Spectra of 1,4-Cyclohexadiene and 1,3-Cyclohexadiene: A Combined Experimental and Theoretical Investigation

Manuela Merchán and Luis Serrano-Andrés

Departamento de Química Física, Universitat de València, Dr. Moliner 50, Burjassot, E-46100 Valencia, Spain

Lee S. Slater and Björn O. Roos*

Department of Theoretical Chemistry, Chemical Centre, P.O.B. 124, S-221 00 Lund, Sweden

Ruth McDiarmid and Xing Xing

Laboratory of Chemical Physics, National Institute of Diabetes and Digestive and Kidney Diseases, National Institutes of Health, Bethesda, Maryland 20892

Received: April 19, 1999

The electronically excited states of the two isomers 1,3- and 1,4-cyclohexadiene are examined by means of multiconfigurational second-order perturbation (CASPT2) theory with extended ANO-type basis sets. The calculations comprise the lower valence excited states plus all singlet 3s, 3p, and 3d members of the Rydberg series converging to the first ionization limit for the 1,3 isomer and the two first limits for 1,4. Companion optical and resonantly enhanced multiphoton ionization spectroscopic measurements were made on the 1,3 isomer. The computed vertical excitation energies were found to be in agreement with the available experimental energies for both systems. New assignments are proposed on the basis of combined experimental and theoretical efforts.

1. Introduction

The cyclic nonconjugated 1,4-cyclohexadiene and conjugated 1,3-cyclohexadiene have been of experimental and theoretical interest for understanding the electronic structures and photophysics of molecules with interacting double bonds. The interaction of unconjugated π-electron systems is usually described in terms of two distinct symmetry-controlled mechanisms: (i) direct through-space (TS) overlap and (ii) through-bond (TB) or hyperconjugative interaction.[1] The model for optimal hyperconjugation is planar 1,4-cyclohexadiene, where the double bonds are almost totally uncoupled by the presence of the methylene groups. The TB interaction leads to destabilization of the in-phase with respect to the out-of-phase combination of the bonding and antibonding ethylenic π MOs, yielding an inverted level ordering. In contrast, norbornadiene, a model for systems where through-space interaction dominates, shows normal ordering with the plus combination of the bonding (and antibonding) ethylenic MOs at lower energy. A normal ordering is also found in conjugated dienes like *cis*-1,3-butadiene and cyclic dienes like 1,3-cyclopentadiene. We have previously shown that the electronic spectra of *cis*-1,3-butadiene (CB),[2] 1,3-cyclopentadiene (CP), aromatic five-membered heterocycles (pyrrole, furan, thiophene),[3,4] norbornadiene (NB),[5] and methylenecyclopropene[6] can be explained on the same basic grounds, as resulting from the interaction between the two double bonds. In this work we shall extend the model for two interacting double bonds by studying the electronic spectra in vacuo of 1,3-cyclohexadiene (CHD13), involved in photochemical processes of current interest, and 1,4-cyclohexadiene (CHD14), the archetype system where the TB coupling overcomes TS interaction.

The optical absorption spectrum of CHD14 shows a weak structure starting around 6 eV, which progressively increases in intensity to a maximum near 8.1 eV. A strong sharp band near 7.4 eV is superimposed on the broad absorption.[7] In the electron impact investigation reported by McDiarmid and Doering,[8] the expected inverted level ordering was demonstrated for CHD14 based on the observed forbidden and allowed p-Rydberg and valence transitions, and on the corresponding selection rules. They were able to characterize a number of valence and Rydberg features. In addition, the symmetry of Rydberg transitions in CHD14 has been studied by using multiphoton ionization techniques.[9] Information about the lowest triplet states is available from the electron impact study performed by Frueholz et al.[10] The only previous theoretical ab initio study of this molecule known to us is the RPA calculation of Galasso from 1991.[11]

Optical[12] and electron impact[10] spectroscopies describe a different structure for the spectrum of CHD13. Intense transitions peak at 4.94 eV and near 7.8 eV with several intermediate sharp bands.[10] In contrast to the 1,4 isomer, this spectrum is similar to the spectra of the other *cis*-diene systems, such as 1,3-cyclopentadiene, furan, and pyrrole.[3] The vertical energy of the $^1A_1$ dark state, traditionally believed to play a relevant role in the UV-induced electrocyclic ring opening of CHD13 to 1,3,5-hexatriene,[13,14] a prototypical pericyclic reaction, has been inferred to lie near 6.2 eV.[13] Two ab initio studies of the excited states of CHD13 have been reported. One, a MRCI calculation by

10.1021/jp991266z CCC: $18.00
Published on Web 06/25/1999

TABLE 1: CASSCF Wave Functions (Four Active Electrons) Employed To Compute the Valence and Rydberg Excited States of 1,4-Cyclohexadiene (D_{2h} Symmetry) and 1,3-Cyclohexadiene (C_2 Symmetry)

active space[a]	state labels	states[b]	config.[c]	N_{states}[d]
		1,4-Cyclohexadiene		
00002111	^1A_g	H → $3p_z$, V_5	17	3
00002111	^3A_g	H → $3p_z$	9	1
00002111	$^1B_{2u}$, $^3B_{2u}$	H − 1 → $3p_z$	11(12)	1(1)
00001121	^1A_g, ^3A_g	H − 1 → $3d_{yz}$	17(9)	3(1)
00001121	$^1B_{2u}$, $^3B_{2u}$	H → $3d_{yz}$	11(12)	1(1)
00001211	$^1B_{3u}$	H → $3d_{xz}$, V_2, V_4	11	3
00001211	$^3B_{3u}$	T_1, H → $3d_{xz}$, T_3	12	3
00001211	$^1B_{1g}$	H − 1 → $3d_{xz}$, V_1, V_3	11	4
00001211	$^3B_{1g}$	T_2, H − 1 → $3d_{xz}$, T_4	12	3
30001111	$^1B_{1u}$, $^3B_{1u}$	H → 3s, $3d_{z^2}$, $3d_{z^2-y^2}$	23(27)	3(3)
30001111	$^1B_{3g}$, $^3B_{3g}$	H − 1 → 3s, $3d_{z^2}$, $3d_{x^2-y^2}$	23(27)	3(3)
00101111	$^1B_{1u}$, $^3B_{1u}$	H − 1 → $3p_y$	5(6)	1(1)
00101111	$^1B_{3g}$, $^3B_{3g}$	H → $3p_y$	5(6)	1(1)
01001111	$^1B_{2g}$, $^3B_{2g}$	H → $3p_x$	5(6)	1(1)
01001111	^1A_u, ^3A_u	H − 1 → $3p_x$	5(6)	1(1)
00011111	$^1B_{2g}$, $^3B_{2g}$	H − 1 → $3d_{xy}$	5(6)	1(1)
00011111	^1A_u, ^3A_u	H → $3d_{xy}$	5(6)	1(1)
		1,3-Cyclohexadiene		
72	^1A	H → 3s, $3d_{z^2}$, $3d_{x^2-y^2}$ $3p_z$, $3d_{xy}$, V_2, V_4	302	8
72	^3A	T_1, H → 3s	322	2
36	^1B	H → $3p_x$, $3p_y$, $3d_{xz}$, $3d_{yz}$ V_1, H − 1 → 3s, V_4 (12)[e]	258	15
36	^3A	T_2	324	1

[a] Orbital labeling: D_{2h} (a_g, b_{3u}, b_{2u}, b_{1g}, b_{1u}, b_{2g}, b_{3g}, a_u); C_2 (a, b). [b] CASSCF state ordering and main character of the state. [c] Number of CSFs (within parentheses for the triplet states). [d] Number of state-averaged CASSCF roots (within parentheses for the triplet states). [e] 12th CASSCF root.

Share et al.,[15] placed the intense transition to the first valence ^1B state (at the ground state geometry) at much higher energies than the weak transition to the lowest valence excited ^1A state.[16] The other[17] placed the B vertically excited state below the A state.

The theoretical study of the electronic spectra presented here has been performed within the framework of multiconfigurational second-order perturbation CASPT2 theory,[18,19] which in a number of earlier applications (see, e.g., refs 20 and 21) has been used successfully for computing differential correlation effects for excitation energies. New optical and resonant-enhanced multiphoton ionization spectra of 1,3-CHD have been measured and analyzed. The optical and electron impact spectra of 1,4-CHD have been reanalyzed. Excellent agreement has been found between computed and experimental vertical transition energies.

2. Theoretical Methods and Computational Details

The ground state geometries of 1,4- and 1,3-cyclohexadiene were optimized at the CASSCF level of theory (four active MOs/four active electrons) using atomic natural orbital (ANO) type basis sets[22] contracted to 4s3p1d functions for carbon and 2s1p functions for hydrogen. The vertical excitation energies were computed with the same basis set supplemented with an optimized set of 1s1p1d Rydberg-type functions placed in the molecular charge centroid and derived according to a procedure, which has been explained elsewhere.[20]

Table 1 compiles the details of the CASSCF calculations performed on both systems. Active spaces, character of the states, number of CSF's (configuration state functions), and number of state-averaged CASSCF roots employed for each type of states are summarized. The high symmetry of the 1,4 isomer makes it possible to partition the active orbital spaces for the different states to a larger extent than in the case of the 1,3 isomer. In all cases four active electrons were considered in the active spaces, which include the four valence π,π^* orbitals plus selected sets of Rydberg orbitals. All excitation energies were obtained using the ground state energy computed with the same active space as was used in the calculation of the corresponding excited states.

The CASPT2 method calculates the first-order wave function and the second-order energy with a CASSCF wave function[23] constituting the reference function. All strongly interacting configurations are included in the wave function at this level of theory, and the dynamic correlation energy is obtained by the second-order perturbation treatment. Other properties are obtained from the CASSCF wave function. Recently, a level shift technique was introduced[24] in the CASPT2 approach, which can be used to remove the effect of weakly interacting intruder states.[24,25] The method has been given the acronym LS-CASPT2. There was no need to use a level shift for the 1,4-isomer with its high symmetry, but for 1,3-cyclohexadiene a level shift of 0.3 au had to be used to remove the effect of intruder states. The transition dipole moments, obtained using the CAS state interaction (CASSI) method,[26] were combined with energy differences calculated at the CASPT2 level in order to obtain oscillator strengths.

All calculations have been performed with the MOLCAS−3[27] program package.

3. Experimental Methods

The experimental techniques have been described earlier.[28] Briefly, the optical absorption spectrum of gaseous samples at room and solid CO_2 temperatures were measured in a Cary 15 spectrophotometer. The instrument resolution, approximately 10 cm^{-1}, is smaller than the experimental bandwidth. The quantity of sample in the cell was between 5 and 15 Torr·cm.

The resonant-enhanced multiphoton ionization (REMPI) spectra were measured on a conventional supersonic molecular beam coupled with a time of flight mass spectrometer, also previously described.[28] In the current experiments, 1−3 atm of Ar was seeded with 10−30 Torr of 1,3-cyclohexadiene. In one experiment, approximately 400 Torr butane was added to the seeding gas to reduce the vibrational temperature of the sample molecules. Under these experimental conditions, the parent ion was not observed. In most experiments the spectrum of C_2H_2, the dominant fragment, was recorded. Around 410 nm and around 505 nm, the assumed mass independence of the REMPI spectrum of 1,3-CHD was verified. Spectra were obtained by exciting with both circularly and linearly polarized light, but the comparisons were not informative. Several laser dyes were used to cover the wavelength regions of interest. Room temperature REMPI and photoacoustic (PA) spectra were measured on 1−30 Torr static samples.

1,3-Cyclohexadiene, butane, and argon were commercial samples. The CHD was vacuum distilled when used.

4. Experimental Results and Analysis

4.1. 1,4-Cyclohexadiene. No new experimental measurements were made on 1,4-cyclohexadiene (CHD14). However, for this study the original electron energy loss spectrum[8] and the original optical spectrum[29] were reexamined. The diffuse parameter-dependent electron scattering intensity around 5.8−6.2 eV is observed to be absent from the optical spectrum, thus enabling underlying sharp bands to be detected here. The diffuse

scattering, centered around 5.8 eV, retains its assignment as arising from a forbidden valence transition. The lowest frequency band that appears in the optical spectrum is a sharp band approximately 800 cm^{-1} to the blue of the previously unassigned, apparently parameter-sensitive, 6.1 eV electron scattering band (bands to the red of 49 000 were not reported). It seems reasonable to assign this as a vibrational overtone of the 6.1 eV electron impact band and, because of its sharpness, to assign it as a Rydberg ← X transition. It is most likely the 3s Rydberg ← X transition and appears parameter-dependent in the electron impact spectrum because it is superimposed on a diffuse, forbidden, valence transition. The next sharp optical band lies ≈230 cm^{-1} to the blue of the 6.42 eV band previously assigned as a 1-photon forbidden 3p Rydberg ← X transition converging on the first ionization potential.[9] Presumably, the optically active band is a false origin to this 3p Rydberg band. Because the most likely enabling vibration is the 250 cm^{-1} torsion[30] and the most likely intensity donating transition is one of the intense B_{3u} valence transitions, the 6.42 eV 3p Rydberg ← X transition is assigned B_{3g}. To the blue of this transition is a diffuse optical band at approximately the same energy as the previously unassigned, parameter-sensitive 6.65 eV electron impact band. The optical band has a weak shoulder, ≈300 cm^{-1} to its red. We assume that the stronger band is an optical false origin to the weaker. On the basis of its effective quantum number this band could arise from a 3p Rydberg ← X transition converging on the first ionization potential ($n^* = 2.50$) or a 3s Rydberg ← X transition converging on the second ionization potential ($n^* = 2.05$; $IP_1 = 8.82$ eV, $IP_2 = 9.88$ eV[31,32]). The enabling mode for this forbidden transition is most likely also the 250 cm^{-1} torsion. The intensity donating transition is probably one or both of the intense B_{3u} valence transition. Thus the 6.65 eV transition is also B_{3g}. Because the B_{3g} 3p Rydberg state converging on the first ionization potential has already been assigned, by elimination the 6.65 eV transition can now be assigned as the B_{3g} 3s Rydberg transition converging on the second ionization potential. The remaining transitions in the spectra are, as before, a broad band around 7.0 eV previously assigned as an allowed valence transition, a very strong and sharp band at 7.3 eV previously assigned as a 3p Rydberg transition converging on the second ionization potential, and the very strong allowed valence transition centered around 7.75 eV.

4.2. 1,3-Cyclohexadiene. The electronic spectrum of CHD13 between 4 and 10 eV has been previously published.[8,10] The angle-variation electron impact spectrum was studied to see if additional singlet excited states could be detected. No additional bands to those previously observed were found.[33]

The optical spectrum of gaseous CHD13 was measured at solid CO_2 temperature. The absorption of the broad 4.74 eV (280−210 nm) band was as before.[8] It will not be presented. The absorption spectrum of the 210−190 nm (5.9−6.5 eV) wavelength region is presented in the lower half of Figure 1. At this temperature, unlike in the lower resolution electron impact or the room temperature optical absorption spectra, the two main peaks are seen to be composed of, or have superimposed on them, a large number of closely separated sub-bands. These sub-bands appear as weak inflections on the red side of the main bands and as relatively sharp peaks at the maxima and on the blue side. The two main peaks are separated by approximately 1450 cm^{-1}. Additional very weak bands, separated by approximately 190 cm^{-1}, are observed far to the red of the first structured band.

REMPI spectra of jet-cooled CHD13 were measured in the 450−550 nm (5.5−4.5 eV) and 390−425 nm (6.3−5.8 eV) regions. The former was chosen because the experimental wavelength is twice that of $\pi\pi^*$ the valence and the N → 3s Rydberg transitions. The latter was chosen to aid in interpreting the peculiar spectrum of the 210−190 nm energy region. These spectra are presented in Figure 2 and in the upper half of Figure 1, respectively.

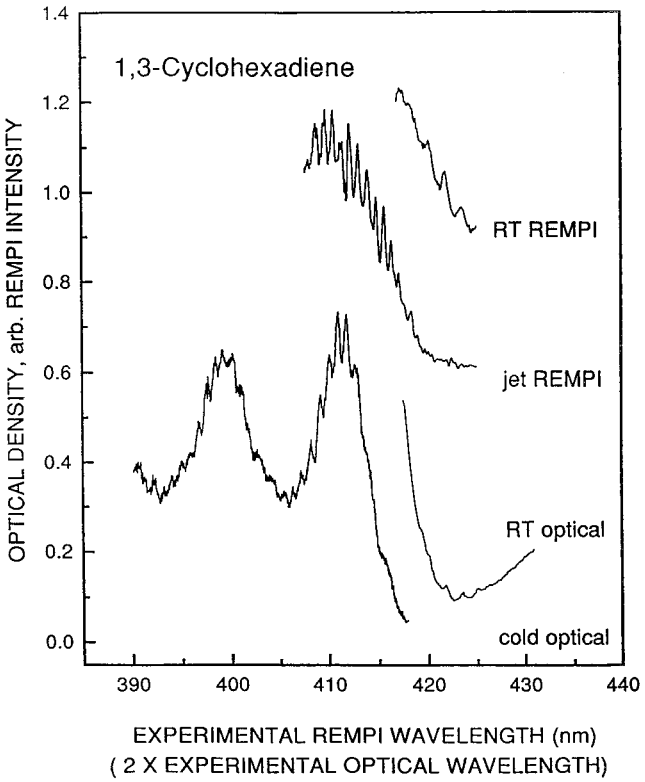

Figure 1. Optical (lower) and (2+1) REMPI (upper) spectra of 1,3-cyclohexadiene. The experimental wavelength of the optical spectrum has been multiplied by 2 to correspond to the wavelength of the REMPI spectrum. The "cold" optical spectrum is at solid CO_2 temperature.

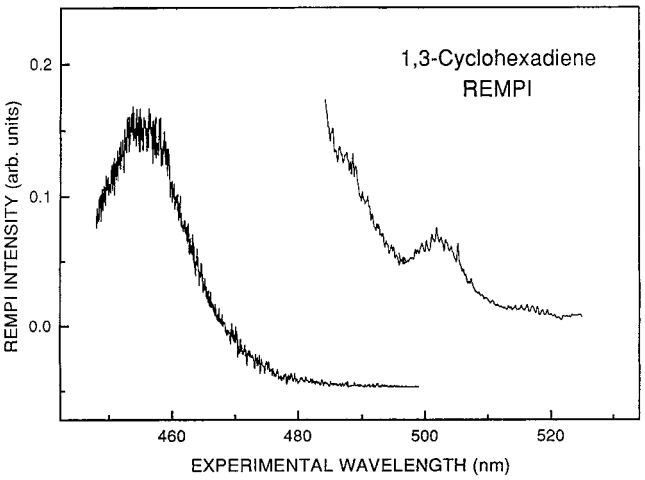

Figure 2. REMPI spectrum of 1,3-cyclohexadiene. See text for number of resonant photons.

In the 450−550 nm experimental region it was not possible to experimentally determine the number of resonant photons because the parent ion of CHD was not observed. However, because the ≈460 nm band is so much more intense than either the ≈520 or ≈505 nm bands, the former is assigned as arising from 2 photon and the latter from 3 photon resonances. The experimental wavelengths thus correspond to transition energies

of 230, 173, and 168 nm (5.39, 7.16, and 7.38 eV), respectively. The two higher energy bands appear to be composed of, or are superimposed on by, narrowly spaced sub-bands. The 5.39 eV band is extremely broad and unstructured and lies under the broad 4.74 eV band in the optical and electron impact spectra. The 7.16 and 7.38 eV bands correspond in energy to bands observed in the electron impact spectrum. On the basis of their effective quantum numbers (5.39 eV = 2.16, 7.16 eV = 3.52, and 7.38 eV = 3.92 (IP, 8.25 eV[34])) it seems reasonable to assign these bands as arising from the 3s, one of the 4p, and one of the 4d Rydberg ← X transitions, respectively.

The REMPI spectrum between 420 and 390 nm is similar to the optical spectrum of the corresponding energy region, 210−190 nm (cf. Figure 1): they each manifest two intense, broad bands with superimposed fine structure. REMPI and PA measurements on room temperature samples of CHD13 find very weak bands far to the red of the main bands, as in the optical spectrum. However, the REMPI and optical spectra differ by the presence of a more extensive substructure on the red side of each main band in the REMPI spectrum than in the optical spectrum and the exact positions of the maxima of the main peaks. There are two experimental differences between the REMPI and optical experiments that might give rise to the observed differences. The optical and REMPI experiments differ in the number of resonant photons and in the temperatures of the samples. The sample temperature for the optical measurement was an equilibrium −80 °C. The sample temperature for the REMPI measurements was the nonequilibrium temperature of a jet-cooled sample. Under our expansion conditions, the rotational temperature of the jet-cooled sample was around 10° and the vibrational temperatures were probably near or at room temperature. To test whether the warmer vibrational temperature of the sample in the REMPI experiment might be the source of the observed spectral difference, one REMPI measurement was made on CHD13 coexpanded with Ar plus butane. Between the experimental wavelengths of 410 and 420 nm, the spectra obtained with and without butane in the sample mixture were the same. Thus, differences in the sample vibrational temperatures is not the cause of the difference between the REMPI and optical spectra in this energy region. The spectral difference, therefore, must be related to the number of absorbed photons. We will return to this issue below.

The very weak bands observed to the red of the main bands in the room temperature (2+1) REMPI and PA spectroscopic measurements merged irregularly into the bands observed in the spectrum of the jet-cooled sample. Because the far red bands are separated by ≈200 cm^{-1}, which is the lowest ground state vibrational frequency of CHD13,[35] and several such bands are observed, excited CHD13 is deduced to distort along this ring deformation and ═C−C═ single bond torsion coordinate. A long Franck−Condon progression in this mode is thus expected and the band origin is predicted to be relatively weak, as was observed for norbornadiene.[28] The stronger bands are separated by ≈100 cm^{-1}. Because the second lowest vibrational frequency of CHD13 is ≈300 cm^{-1},[35] we propose that the 100 cm^{-1} intervals are the differences between torsional modes built on the origin and torsional modes modes built on a +300 false origin. The origin of the (2+1) REMPI active transition is estimated to lie ≈200 cm^{-1} to the red of the first 100 cm^{-1} interval, around 5.92 eV. Its vertical transition is observed around 6.05 eV. Three vibrational modes, 200, 300, and 1450 cm^{-1}, are assigned in the excited state. The effective quantum number of this REMPI transition is 2.44. Because this transition is 1-photon inactive and 2-photon active, it is assigned as the A $3p_z$ ← X Rydberg transition. It is A_2 in the full C_{2v} symmetry of planar CHD13 and is therefore expected to be weak.

The question now remains as to whether or not the transition observed in the optical and 2-photon resonant spectra are the same. If the same criteria that was used to assign the origin of the 2-photon resonant transition is applied to the optical spectrum, the origin of the optical transition is estimated to lie at 5.89 eV. The maximum of this transition is 6.03 eV. While the displacements of these energies from those of the 2-photon resonant transition are small, the differences lie outside our cumulative calibration errors. The two sets of bands also look different. The absence of vibrational substructure on the red side of the optical spectrum in conjunction with its presence on the blue—high energy—side of the spectrum is itself indicative of another difference between the 1- and 2-photon resonant spectra. Such vibrational substructure can arise only from a local perturbation of the potential energy curve of the upper state of this transition, a perturbation that is absent from the upper state of the 2-photon transition. It thus seems reasonable to assign the optical and 2-photon resonant signals as arising from two different electronic transitions. The optical transition has an effective quantum number of 2.48. It is assigned as one of the 3p B ← X Rydberg transitions.

Higher energy transitions observed before[10] but not assigned appear at 6.68, 6.87 (stronger), 7.20, 7.41, 7.74, and ≈7.85 eV. The 7.2 and 7.4 eV transitions observed in the REMPI spectrum are assigned above.

In summary, five electronic transitions of CHD13 have been identified in this investigation. Three of these have been observed in the electron impact spectrum, the 7.16 and 7.38 high-energy transitions and the 6.03 eV 1-photon active transition. Two additional transitions are reported here, at 5.39 and 6.03 eV. The latter appears to be optically forbidden. Additional bands are observed at 6.68, 6.87, 7.74, and 7.85 eV in the electron impact spectrum.

5. Theoretical Results and Discussion

We present in this section results on the geometry determination and singlet−singlet and singlet−triplet spectra obtained for the nonconjugated CHD14 molecule and the conjugated CHD13 system. Comparisons to previous theoretical studies and to the previous and the present experimental results are also included. Finally, an analysis is performed of the similarities and differences between the spectrum of 1,4-cyclohexadiene and norbornadiene, and 1,3-cyclohexadiene and other conjugated dienes.

5.1. Geometry Determinations. The geometries employed in the study of the electronic spectra of the hexadienes have been determined at the π -CASSCF level (four active MOs/four active electrons). The ANO-L valence basis set C[4s3p1d]/H[2s1p] was used. The equilibrium geometries, together with the available experimental data, are compiled in Table 2.

Geometry optimization at the π-CASSCF level led to a planar structure with D_{2h} symmetry for CHD14, in agreement with the experimental Raman investigation performed by Carreira et al.[36] Computed bond distances and angles are in agreement with the electron diffraction (ED) results.[37,38] The present results also confirm previous theoretical conclusions, obtained at the SCF level, concerning the planarity of the CHD14 system,[39] even if an accurate prediction of the equilibrium geometry cannot be made at this level of theory. Typical is that the SCF value for the C_2═C'_2 bond length is 0.02 Å too short (using the same ANO basis set). In order to check the influence of the dynamic correlation effects on the geometry of CHD14, a geometry

TABLE 2: Optimized (CASSCF) and Experimental Geometries for the Ground State of 1,4-Cyclohexadiene (D_{2h}) and 1,3-Cyclohexadiene (C_2)

parameter	theor CASSCF	electron diffraction (ED) data ref 38	ref 37	ref 43
		1,4-Cyclohexadiene		
$r(C_1-C_2)$	1.504	1.511	1.496	
$r(C_2=C_2')$	1.337	1.347	1.334	
$r(C_1-H_1)$	1.091	1.096	1.114	
$r(C_2-H_2)$	1.077	1.079	1.103	
$\angle(C_2'C_2C_1)$	123.6	122.7	123.4	
		1,3-Cyclohexadiene		
$r(C_1-C_1')$	1.472	1.468	1.468	1.465
$r(C_1=C_2)$	1.343	1.350	1.339	1.348
$r(C_2-C_3)$	1.511	1.523	1.494	1.519
$r(C_3-C_3')$	1.533	1.534	1.510	1.538
$r(C_1-H_1)$	1.075	1.082	1.07	1.099
$r(C_2-H_2)$	1.076	1.082	1.07	1.099
$r(C_3-H_3)$	1.086	1.096	1.14	1.111
$r(C_3-H_4)$	1.091	1.096	1.14	1.111
$\angle(C_1'C_1C_2)$	120.5	120.1	121.6	120.3
$\angle(C_1C_2C_3)$	120.6	120.1	118.2	120.3
$\angle(C_2C_3C_3')$	111.8	110.7	111.5	110.9

Cartesian Coordinates (au)

atom	*X*	*Y*	*Z*
	1,4-Cyclohexadiene		
C1	2.838077	0.000000	0.000000
C2	1.263190	2.366782	0.000000
C1	1.36499	−0.265708	−2.333547
H1	4.087716	0.000000	1.639232
H2	2.264536	4.139006	0.000000
	1,3-Cyclohexadiene		
C2	2.675726	−0.266621	−0.160165
C3	−1.396615	−0.383388	2.307716
H1	2.290193	−0.636943	−4.104582
H2	4.683182	−0.587703	−0.167109
H3	−2.365290	0.515211	3.878278
H4	−1.553770	−2.418106	2.608051

optimization was also made at the MP2 level. The MP2 optimal parameters for the carbon−carbon bond differ at most 0.003 Å from the π -CASSCF results. This is typical and reflects the fact that a π active CASSCF calculation balances two effects: the too short bonds resulting from lack of correlation in the σ-framework and the too long bonds obtained due to the lack of dynamic correlation for the π-electrons.

A parallel study was performed for the CHD13 system. A nonplanar structure with C_2 symmetry was found for CHD13 at the π-CASSCF level (and confirmed at the MP2 level), which is in agreement with the results obtained in the Raman study (the barrier to planarity was estimated to be 0.14 eV).[36] As can be seen in Table 2, the computed geometrical parameters agree with the electron diffraction data and actually fall in between the different measured values for most bond distances and bond angles.

5.2. Electronic Spectrum of 1,4-Cyclohexadiene. The results obtained for CHD14 are collected in Table 3. The first column identifies the different excited states. The second and third columns give the vertical transitions energies computed at the CASSCF and CASPT2 level, respectively. Column 4 contains the experimental transition energies according to assignments made from the analysis of the experimental spectrum. The last column gives the computed oscillator strengths.

The most intense features of the computed singlet−singlet spectrum are related to transitions of valence character. For a qualitative description of the valence electronic transitions it is helpful to consider the interaction of two independent ethylenic

TABLE 3: Computed Vertical Excitation Energies and Oscillator Strengths for 1,4-Cyclohexadiene[a]

state	excitation energies CASSCF	CASPT2	exp	osc str
singlet excited states				
$1^1B_{1g}(V_1)$	9.37	5.74	5.80[b]	forbidden
$1^1B_{1u}(H \rightarrow 3s)$	6.76	5.90	6.10[b]	0.0106
$1^1B_{3g}(H \rightarrow 3p)$	7.24	6.53	6.42[b,d]	forbidden
$1^1B_{2g}(H \rightarrow 3p)$	7.21	6.57		forbidden
$2^1B_{3g}(H-1 \rightarrow 3s)$	7.29	6.67	6.65[d]	forbidden
$2^1A_g(H \rightarrow 3p)$	7.31	6.72		forbidden
$1^1B_{3u}(V_2)$	10.47	7.16	≈7.05[b]	0.2591
$2^1B_{1u}(H \rightarrow 3d)$	7.75	7.16		0.0005
$1^1A_u(H \rightarrow 3d)$	7.71	7.16		forbidden
$3^1B_{1u}(H \rightarrow 3d)$	7.74	7.19		0.0195
$4^1B_{1u}(H-1 \rightarrow 3p)$	7.75	7.22	7.30[b]	0.0234
$2^1B_{3u}(H \rightarrow 3d)$	8.27	7.24		0.0029
$1^1B_{2u}(H \rightarrow 3d)$	7.83	7.35		0.0035
$2^1B_{1g}(V_3)$	11.47	7.41		forbidden
$2^1A_u(H-1 \rightarrow 3p)$	7.78	7.44		forbidden
$2^1B_{2u}(H-1 \rightarrow 3p)$	7.77	7.45		0.0120
$3^1B_{3u}(V_4)$	10.89	7.49	7.75[b]	0.8596
$3^1B_{3g}(H-1 \rightarrow 3d)$	8.27	7.92		forbidden
$2^1B_{2g}(H-1 \rightarrow 3d)$	8.24	7.96		forbidden
$4^1B_{3g}(H-1 \rightarrow 3d)$	8.30	8.03		forbidden
$3^1B_{1g}(H-1 \rightarrow 3d)$	8.78	8.03		forbidden
$3^1A_g(H-1 \rightarrow 3d)$	8.46	8.08		forbidden
$4^1A_g(V_5)$	8.80	8.83		forbidden
triplet excited states				
$1^3B_{3u}(T_1)$	5.03	4.08	4.29[c]	
$1^3B_{1g}(T_2)$	4.95	4.11		
$1^3B_{1u}(H \rightarrow 3s)$	6.71	5.83		
$2^3B_{3u}(T_3)$	10.76	6.21		
$2^3B_{1g}(T_4)$	11.00	6.41		
$H \rightarrow 3p$	7.20−7.23	6.51−6.60		
$2^3B_{3g}(H-1 \rightarrow 3s)$	7.25	6.61		
$H \rightarrow 3d$	7.70−8.16	7.13−7.32		
$H-1 \rightarrow 3p$	7.73−7.77	7.18−7.44		
$H-1 \rightarrow 3d$	8.23−8.81	7.91−8.09		

[a] Previous experimental findings are also included. Energies given in eV. [b] Electron impact spectrum.[8] [c] Electron impact spectrum.[10] [d] This investigation.

moieties. The interaction of the degenerate bonding, π_b, and antibonding, π_a, molecular orbitals of two ethylenic units results in the following MOs: $\pi_1 = \pi_b - \pi_b$, $\pi_2 = \pi_b + \pi_b$, $\pi_3 = \pi_a - \pi_a$, and $\pi_4 = \pi_a + \pi_a$. They lead to the orbital ordering $1b_{3g}(\pi_1)$, $2b_{1u}(\pi_2)$, $1a_u(\pi_3)$, and $2b_{2g}(\pi_4)$ of the D_{2h} point group. As explained in the Introduction, this ordering is the result of the hyperconjugative interaction between the π-system and the methylene groups. The computed SCF orbital energies are −9.80 (H − 1), −9.06 (H), +4.07 (L), and +4.87 eV (L + 1), respectively (H, highest occupied molecular orbital; L, lowest unoccupied molecular orbital). Based on this structure, four singly excited valence singlet states can be expected. In addition, the doubly excited state $(H)^2 \rightarrow (L)^2$, which can be expected to appear in the same energy region, has also been included.

The lowest singlet excited state is of B_{1g} symmetry (V_1 in Table 3). That the lowest singlet−singlet transition is optically forbidden has been clearly established by McDiarmid and Doering.[8] The vertical excitation energy calculated at the CASPT2 level, 5.74 eV, is in agreement with the observed value, 5.80 eV. The $1^1B_{1g}(V_1)$ state is described mainly by the one-electron promotion H → L (93%) in the CASSCF wave function. The second valence excited state is the $^1 1B_{3u}(V_2)$ state, which is calculated at 7.16 eV. In terms of the corresponding natural orbitals, it is described mainly by the one-electron H − 1 → L promotion. The computed oscillator strength is 0.26. The $^2 1B_{1g}(V_3)$ and $3^1B_{3u}(V_4)$ valence states are found within the energy range 7.4−7.5 eV with optically forbidden and strongly allowed

character, respectively. Analysis of the CASSCF wave function indicates that each state is well represented by a single configuration: the H − 1 → L + 1 (94%) for V_3 and the H → L + 1 (95%) for V_4. That the two $^1B_{3u}$ states, V_2 and V_4, do not mix to form the normal minus and plus combinations, with an only weakly allowed minus state and a strongly allowed plus state, is unusual and in contrast to the situation for 1,3-cyclohexadiene and other similar systems like norbornadiene, *cis*-butadiene, and cyclopentadiene.[20,21] By contrast, the corresponding triplet states are heavily mixed. The separations of the two sets of states directly illustrate this unusual situation: the two singlet states are calculated to be separated by 0.33 eV, the triplet states by 2.13 eV. As indicated by the orbital energies, the interacting configurations are as degenerate in CHD14 as they are in the other molecules mentioned above, they just do not interact in the singlet state. A more detailed comparison between different systems with interacting double bonds will be given in the Discussion. The stronger oscillator strength of the fourth transition compared to the second one can be related to the relative phases of the molecular orbitals involved in the transition moments. A rough estimate gives a dipole integral proportional to $1 - S_{12}$ for the lower state and $1 + S_{12}$ for the upper state, where S_{12} is the overlap integral between the two π−orbitals on the carbon atoms connected via the methyl bridge.

The V_2 and V_4 states are consistent by symmetry, transition type, and excitation energy with the assignment of the observed features in the electron impact spectra at ≈7.05 and 7.75 eV, respectively.[8] The deviation from the experimental data is somewhat larger for the most intense transition, which is computed 0.26 eV below the maximum of the observed band at 7.75 eV. Alternately, it may be that the experimental spectrum indicates a somewhat larger V_2−V_4 mixing than is found in the numerical calculation, although the experimental singlet state separation (≈0.7 eV) is still much smaller than was calculated for the triplet states of CHD14.

The doubly excited state $4^1A_g(V_5)$ is calculated to appear at 8.83 eV, which is close to the first ionization limit for CHD14, 8.82 eV.[31,32] This is more than 1 eV higher than the corresponding state in norbornadiene, where it appears at 7.49 eV,[5] and results from the larger H−L splitting in CHD14. The state is dominated by doubly excited configurations with the $(H)^2 \rightarrow (L)^2$ configuration contributing 26% to the CASSCF wave function. The effect of dynamic correlation (the difference between the CASPT2 and CASSCF energies) on the excitation energy is much smaller for this state, which is dominated by covalent structures, than it is for the singly excited states with their large ionic character. It is therefore not surprising that theoretical treatments that do not appropriately include dynamic correlation effects will not yield results of predictive accuracy. This is, for example, evident from the study of CHD14 performed with the random phase approximation (RPA).[11] In the latter, the computed excitation energies are 1−2 eV too large and the intensity ordering is incorrect.

Due to the close spacing of the H and H − 1 MOs, Rydberg states leading to the two ionization limits are expected to overlap in energy even for the early members of the series. The separation of the two lowest IPs is 1.1 eV[31,32] and the separation between the lowest Rydberg states should be smaller. This is also born out by the calculation, which places the H − 1 → 3s state at 6.67 eV, 0.77 eV above the 5.9 eV H → 3s state. The experimental work presented above, in which the H → 3s Rydberg state is located at 6.1 eV and the H − 1 → 3s state at 6.65 eV, is in agreement with these results. Surrounding the second 3s Rydberg state we find the first set of 3p states, in the energy region 6.53−6.72 eV. The 6.42 eV experimental band has been assigned as the B_{3g} 3p Rydberg ← X transition calculated at 6.53 eV. This band was previously assigned as a forbidden transition on the basis of the 2-photon resonant ionization spectrum.[9] In the region between 7.1 and 7.4 eV we find the five members of the first 3d series, surrounding the first member of the second 3p series, located at 7.22 eV, which is assigned to the electronically allowed band observed at 7.30 eV in the EI,[7] and 3-photon REMPI[9] spectra. The transition to the 4^1B_{1u} state at 7.22 eV is computed to have a higher oscillator strength than the transition to the 2^1B_{2u} H − 1 → 3p, Rydberg state at 7.45 eV. The third member of this H − 1 → 3p Rydberg series lies at 7.44 eV and is dipole forbidden. Finally, we find the second 3d series around 8.0 eV.

TABLE 4: Calculated and Experimental Excitation Energies (eV) and Oscillator Strengths for the Excited Singlet and Triplet States of 1,3-Cyclohexadiene

	excitation energies			osc str	
state	CASSCF	CASPT2	exp[a]	calc	exp[a]
$1^1B(V_1)$	8.40	4.72	4.94	0.191	0.12
$2^1A(12a \rightarrow 3s)$	5.83	5.49	5.39[c]	0.003	
$2^1B(12a \rightarrow 3p_x)$	6.43	5.98	6.03[c]	0.032	
$3^1B(12a \rightarrow 3p_y)$	6.50	6.04		0.023	
$3^1A(12a \rightarrow 3p_z)$	6.36	6.12	6.05[c]	0.002	
$4^1A(V_2)$	7.14	6.18	6.3[b]	0.004	
$4^1B(12a \rightarrow 3d_{xz})$	6.98	6.60		0.002	
$5^1A(12a \rightarrow 3d_{x^2-y^2})$	6.83	6.64	6.68[d]	0.0006	
$5^1B(12a \rightarrow 3d_{yz})$	7.07	6.74		0.003	
$6^1A(12a \rightarrow 3d_{z^2})$	6.88	6.75	6.87[d]	0.0001	
$7^1A(12a \rightarrow 3d_{xy})$	6.94	6.82		0.0001	
$6^1B(10b \rightarrow 3s)$	8.79	7.72	7.7	0.070	
$8^1A(V_3)$	11.62	7.77	7.8−7.9	0.354	0.60
$7^1B(V_4)$	14.03	9.27	9.0	0.011	
$1^3B(T_1)$	3.19	2.91	2.94		
$1^3A(T_2)$	5.20	4.79	>4.5		
$2^3A(12a \rightarrow 3s)$	5.72	5.46			

[a] Electron impact,[10] optical,[7] and electron energy loss[12] spectra. [b] Observed in liquid the 1,3-cyclohexadiene spectrum.[7,41] [c] This investigation. [d] Reference 12.

The triplet spectrum is quite different. Here four of the valence excited states occur among the first five states. The two first, $^3B_{3u}$ and $^3B_{1g}$ occur close together at 4.08 and 4.11 eV, respectively. The EI spectrum of Frueholz et al. shows a broad band extending from 3.4 to 5.4 eV with maximum intensity at 4.29 eV.[10] It is clearly a spin-forbidden transition. It is suggested that the band is a superposition of the two transitions N → V_1 and N → V_2, which is in agreement with the present results. No experimental data are available for the higher triplet states.

5.3. Electronic Spectrum of 1,3-Cyclohexadiene. The results obtained for CHD13 are collected in Table 4, including CASSCF and CASPT2 vertical transition energies, oscillator strengths, and experimental transition energies. As in CHD14, the most intense features of the computed singlet−singlet spectrum are related to transitions of valence character. The valence electronic transitions can be understood within the same model as CHD14, as arising from the interaction of two ethylene units. The lower symmetry of the system changes, however, the structure of the orbitals and the character of the interactions. The computed SCF orbital energies are (in eV), 10b(H − 1): −11.4; 12a(H): −8.2; 11b(L): +2.9; 13a(L + 1): +5.7. Unlike CHD14 the second Rydberg series H − 1 → n = 3 is expected at much higher energies than the first because H − 1 is a much deeper orbital. The energies and character of the states will differ from CHD14 because of the different type of interacting double bonds and different symmetry.

The lowest singlet excited state (V_1 in Table 4) peaking between 4.78 eV[16] and 4.94 eV[10] was clearly identified as the lowest valence state of B symmetry. The CASPT2 excitation energy of 4.72 eV is in agreement with the observed value, as is the computed oscillator strength, 0.19, compared to the experimental value of 0.12.[12] The transition has a CASSCF wave function formed mainly by the HOMO → LUMO excitation (90%). As will be discussed below, the decrease in energy with respect to other conjugated *cis*-dienes is related to the hyperconjugative effect.

The CASPT2 calculation places the $2^1A(12a \rightarrow 3s)$ state at 5.49 eV with low oscillator strength. This is supported by the REMPI results presented here. The Rydberg states $2^1B(12a \rightarrow 3p_x)$ and $3^1B(12a \rightarrow 3p_y)$ are located by the CASPT2 method at 5.98 and 6.04 eV, respectively, with similar oscillator strengths (0.03 and 0.02). The $3^1A(12a \rightarrow 3p_z)$ Rydberg state is located at 6.12 eV with a much lower oscillator strength. The present experimental results identify a strongly allowed Rydberg state at 6.03 eV that appears to be weakly perturbed and a strong 2-photon state at 6.05 eV that is not observed in the optical spectrum. The experimental assignment of the latter as $A(3p_z)$ is consistent with its computed transition energy and low oscillator strength. The identification of the former is less clear. Transitions to both B 3p Rydberg states are calculated to lie within 0.06 eV of each other and to have equal intensities, yet only one transition is observed here. By analogy with the situation in 1,3-cyclopentadiene, in which both the 1- and 2-photon transitions to the $^1B_2(3p_y)$ Rydberg state are strong whereas only the 1-photon transition to the $^1B_1(3p_x)$ was observed,[40] we suggest that the 6.03 eV transition observed here is a weakly perturbed transition to the $2^1B(3p_x)$ Rydberg state of CHD13.

Slightly above these states, at 6.18 eV with an oscillator strength of 0.004, the CASPT2 calculation finds the 4^1A valence state. The composition of the CASSCF wave function for this state is H − 1 → L (26%), H → L + 1 (15%), and $(H)^2 \rightarrow (L)^2$ (39%). The low symmetry of the system allows the doubly excited configuration to mix and contribute to this state, unlike in CHD14 (the V_5 state). While no evidence of this state is seen in the gas phase spectra,[16] a transition has been reported[41] near 6.3 eV in the liquid phase. As Rydberg transitions do not appear in solution, the most likely assignment for this transition is to a valence state. This is consistent with the computed V_2 4^1A state at 6.18 eV, close in energy to the corresponding state of other dienes.[24]

Optical,[42] electron energy loss,[12] and electron impact[10] spectroscopies report bands at 6.68 and 6.87 eV. On the basis of their effective quantum numbers, the former probably arises from a transition to one of the Rydberg H → 3d states (cf. Table 4), and the latter to the H → 4s Rydberg state, which has not been calculated here.

The most intense band of the spectrum of CHD13 peaks between 7.8 and 8.0 eV.[7,10,12] A weak bump observed near 0.1 eV below the band maximum, that is at 7.7 eV, can tentatively be assigned to the $6^1B(10b \rightarrow 3s)$ state, computed at 7.72 eV with an oscillator strength 0.07. The strongest band of the spectrum (experimental oscillator strength 0.60) is assigned to the 8^1A $\pi\pi^*$ valence V_3 state, computed at 7.77 eV with an oscillator strength 0.35. The CASSCF wave function of the state has the following composition: H − 1 → L (59%), H → L + 1 (5%), and $(H)^2 \rightarrow (L)^2$ (19%). It is the A^+ state of dienes and polyenes[12] (see below). The observed band is very broad and different valence and Rydberg states are likely to be hidden under it in the low-resolution impact spectrum. We have for instance computed the V_4 valence 7^1B $\pi\pi^*$ state at 9.27 eV with a low oscillator strength. This result is consistent with the observed value of 9.0 eV in the electron energy loss spectrum.[12] In the CASSCF wave function this state is described as mainly the one-electron promotion H − 1 → L + 1 (79%).

Regarding the triplet states, an intensity maximum is found at 2.94 eV in the electron impact spectrum[10] and assigned to a singlet−triplet transition. The CASPT2 excitation energy for the $1^3B(T_1)$ state is 2.91 eV. The state is characterized as the H → L triplet state. The energy of the excitation is consistent with the singlet−triplet energy found in similar *cis*-dienes such as *cis*-1,3-butadiene[2] and 1,3-cyclopentadiene.[3] The second triplet transition is reported by Frueholz et al.[10] higher than 4.5 eV. This observation is consistent with our CASPT2 value for the $1^3A(T_2)$ state at 4.79 eV. The presence of the much more intense V_1 band will undoubtedly obscure the transition to the second triplet valence state.

6. Discussion

In the above sections we have presented the results of experimental and numerical experiments of the excited states of CHD13 and CHD14. Inspection of Tables 3 and 4 shows agreement between both for transition energies and intensities for those states that could be experimentally observed. This agreement has been previously observed for the analogous molecules norbornadiene and cyclopentadiene as well as for the linear polyenes. We are now in a position to use the results of these calculations to rationalize the differences between the excited state manifolds of these molecules in terms of their orbital and state interactions.

The calculated transition energies for CHD14, norbornadiene (NB).[5] CHD13, and 1,3-cyclopentadiene (CP)[3] are presented in Table 5 together with orbital energies and energy differences (the molecules are shown in Figure 3 with the coordinate axes used). State symmetries entered in Table 5 reveal that for CHD14, the V_1 and V_3 and the V_2 and V_4 states are of the same symmetries. By contrast, for NB, CHD13, and CP, it is the V_1 and V_4 and the V_2 and V_3 states that are of the same symmetries. In addition, for CHD14 and NB the symmetric doubly excited valence state does not correspond in symmetry to any of the valence excited states studied, whereas for CHD13 and CP the doubly excited state belongs to the same symmetry as other included valence excited states. Thus different state interactions are expected in the different molecules.

Consider first the comparison of CHD14 and NB. Both molecules lack doubly excited states of the same symmetry as any of the first four valence excited states so their energy manifolds should reflect mainly orbital and state interactions between the states and orbitals displayed in Table 5. For these two molecules the orbital energy differences are smaller for NB than CHD14. In each, the orbital energy differences (H − 1) → L and L → (H + 1) are degenerate. The main difference between the species is that V_2 and V_3, the degenerate states, are of the same symmetry in NB and not in CHD14, so interaction is possible for NB but not for CHD14. The smaller energy differences to each state in NB than CHD14 correlates well with the observed lower transition energies in NB than in CHD14. The energy differences between the two V_2 and V_3 states are calculated to be similar in the two species, despite the symmetry restrictions on mixing in CHD14. From this we conclude that V_2-V_3 mixing is weak in NB. The triplet states of NB are likewise calculated below those of CHD14, although, as was noted in the section describing the results for CHD14, the larger T_1-T_3 splitting in the triplet states of CHD14 than

TABLE 5: Computed CASPT2 Excitation Energies (ΔE in eV) and Computed Oscillator Strengths for the Singlet Valence States and the Two Lowest Triplet States in 1,4-Cyclohexadiene (CHD14), Norbornadiene (NB), 1,3-Cyclohexadiene (CHD13), and 1,3-Cyclopentadiene (CP)

	CHD14			NB			CHD13			CP		
state	label	ΔE	osc str	label	ΔE	osc str	label	ΔE	osc str	label	ΔE	osc str
V_1	$^1B_{1g}$	5.74	forb	$^1A_2$	5.28	forb	^1B	4.72	0.191	$^1B_2$	5.27	0.148
V_2	$^1B_{3u}$	7.16	0.259	$^1B_2^-$	6.20	0.008	$^1A^-$	6.18	0.004	$^1A_1^-$	6.31	0.0003
V_3	$^1B_{1g}$	7.41	forb	$^1B_2^+$	6.48	0.343	$^1A^+$	7.77	0.354	$^1A_1^+$	7.89	0.442
V_4	$^1B_{3u}$	7.49	0.860	$^1A_2$	7.36	forb	^1B	9.27	0.011			
V_5	^1A_g	8.83	forb	$^1A_1$	7.49	0.0002						
T_1	$^3B_{1g}$	4.11		$^3A_2$	3.42		^3B	2.91		$^3B_2$	3.15	
T_2	$^3B_{3u}$	4.08		$^3B_2$	3.80		^3A	4.79		$^3A_1$	4.90	
					SCF Orbital Energies (eV)							
$\epsilon(\pi_4)$		4.87			3.52			5.68			5.65	
$\epsilon(\pi_3)$		4.07			2.44			2.94			3.10	
$\epsilon(\pi_2)$		−9.06			−8.60			−8.16			−8.38	
$\epsilon(\pi_1)$		−9.80			−9.64			−11.43			−11.27	
$D_1 = \epsilon(\pi_3) - \epsilon(\pi_2)$		13.1			11.0			11.2			11.5	
$D_2 = \epsilon(\pi_3) - \epsilon(\pi_1)$		13.9			12.1			14.4			14.4	
$D_3 = \epsilon(\pi_4) - \epsilon(\pi_2)$		13.9			12.1			13.9			14.0	
$D_4 = \epsilon(\pi_4) - \epsilon(\pi_1)$		14.7			13.2			17.1			16.9	

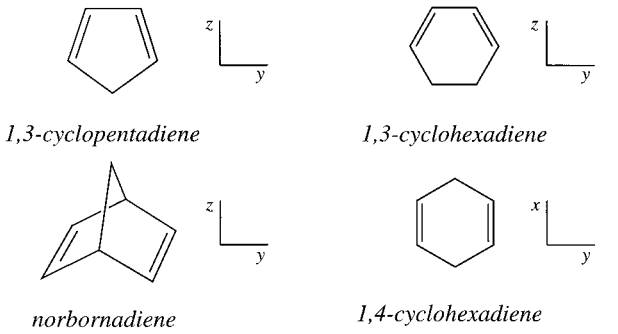

Figure 3.

in the singlet V_2-V_4 separation somewhat masks the orbital energy difference - transition energy trend in these molecules.

A comparison between results obtained for NB and for CHD13 and CP reveals the effect of the symmetric doubly excited state on the valence manifold. All three molecules have similar H → L energy differences and similar transition energies to the V_1 state. For this V_1 state, the orbital energy differences of NB, CHD13, and CP are smaller than those calculated for CHD14 and so are the transition energies. The (H − 1) → L and H → (L + 1) states of each of the three molecules are of the same symmetry, but the orbital energy differences of the states are larger for CHD13 and CP than for NB. In the absence of further interaction, the transition energies to the V_2 and V_3 states of CHD13 and CP are predicted to be larger than those of NB. This is observed for both the singlet V_3 state and the triplet T_2 state of each molecule but not for the singlet V_2 state, where the transition energies of CHD13 and CP are calculated to be similar to that of NB. The failure of the predictions based on simple orbital energy differences is a manifestation of the need to consider configuration interaction in this type of rationalization where permitted by symmetry. Such interaction may be weak, as noted for the V_2 and V_3 states of NB. However, as occurs for CHD13 and CP, it may be strong and necessary to consider.

7. Conclusions

We have presented new experimental data and a theoretical analysis of the electronic spectra for 1,4-cyclohexadiene and 1,3-cyclohexadiene. Optical and resonantly enhanced multiphoton ionization spectroscopic measurements were made on CHD13, and previously measurements for CHD14 were reanalyzed. The theoretical results were based on CASSCF/CASPT2 calculations. The results for transition energies and intensities are in agreement with all available experimental data. The excitation energies can be qualitatively understood in terms of the different types of interaction that takes place between the double bonds of the molecules and the differences in state symmetries. Where interaction between the doubly excited state and the singly excited states is not possible, orbital energy differences dominate the observed spectroscopic trends.

Acknowledgment. The research reported in this communication has been supported by a grant from the Swedish Natural Science Research Council (NFR), by project PB94-0986 of Spanish DGICYT, and by the European Commission through the TMR network FMRX-CT96-0079. Helpful discussions with Professor Werner Fuss are gratefully acknowledged.

References and Notes

(1) Hoffmann, R.; Heilbronner, E.; Gleiter, R. *J. Am. Chem. Soc.* **1970**, *92*, 706.

(2) Serrano-Andrés, L.; Roos, B. O.; Merchán, M. *Theor. Chim. Acta* **1994**, *87*, 387.

(3) Serrano-Andrés, L.; Merchán, M.; Nebot-Gil, I.; Roos, B. O.; Fülscher, M. P. *J. Am. Chem. Soc.* **1993**, *15*, 6184.

(4) Serrano-Andrés, L.; Merchán, M.; Fülscher, M.; Roos, B. O. *Chem. Phys. Lett.* **1993**, *211*, 125.

(5) Roos, B. O.; Merchán, M.; McDiarmid, R.; Xing, X. *J. Am. Chem. Soc.* **1994**, *116*, 5927.

(6) Merchán, M.; González-Luque, R.; Roos, B. O. *Theor. Chim. Acta* **1996**, *94*, 143.

(7) Robin, M. B. *Higher Excited States of Polyatomic Molecules*; Academic Press: New York, 1975; Vol. II.

(8) McDiarmid, R.; Doering, J. P. *J. Chem. Phys.* **1981**, *75*, 2687.

(9) Sabljić, A.; Auerbach, A.; McDiarmid, R. *Int. J. Quantum Chem.: Quantum Chem. Symp.* **1982**, *16*, 357.

(10) Frueholz, R. P.; Flicker, W. M.; Mosher, O. A.; Kuppermann, A. *J. Chem. Phys.* **1979**, *70*, 1986.

(11) Galasso, V. *Chem. Phys.* **1991**, *153*, 13.

(12) McDiarmid, R.; Sabljić, A.; Doering, J. P. *J. Chem. Phys.* **1985**, *83*, 2147.

(13) Trushin, S. A.; Fuss, W.; Schikarski, T.; Schmid, W. E.; Kompa, K. L. *J. Chem. Phys.* **1997**, *106*, 9386.

(14) Reid, P. J.; Doig, S. J.; Wickham, S. D.; Mathies, R. A. *J. Am. Chem. Soc.* **1993**, *115*, 4754.

(15) Share, P. E.; Kompa, K. L.; Peyerimhoff, S. D.; Van Hemert, M. C. *Chem. Phys.* **1988**, *120*, 411.

(16) Share, P. E.; Kompa, K. L. *Chem. Phys.* **1989**, *134*, 429. The experiment undertaken to confirm this result obtained, instead, the spectrum of benzene (R. McDiarmid, unpublished data).

(17) Celani, P.; Bernardi, F.; Robb, M. A.; Olivucci, M. *J. Phys. Chem.* **1996**, *100*, 19364.

(18) Andersson, K.; Malmqvist, P.-Å.; Roos, B. O.; Sadlej, A. J.; Wolinski, K. *J. Phys. Chem.* **1990**, *94*, 5483.
(19) Andersson, K.; Malmqvist, P.-Å.; Roos, B. O. *J. Chem. Phys.* **1992**, *96*, 1218.
(20) Roos, B. O.; Fülscher, M. P.; Malmqvist, Per-Åke; Merchán, M.; Serrano-Andrés, L. Theoretical studies of electronic spectra of organic molecules. In *Quantum Mechanical Electronic Structure Calculations with Chemical Accuracy*; Langhoff, S. R., Ed.; Kluwer Academic Publishers: Dordrecht, The Netherlands, 1995; p 357.
(21) Roos, B. O.; Andersson, K.; Fülscher, M. P.; Malmqvist, P.-Å.; Serrano-Andrés, L.; Pierloot, K.; Merchán, M. Multiconfigurational perturbation theory: Applications in electronic spectroscopy. In *Advances in Chemical Physics: New Methods in Computational Quantum Mechanics*; Prigogine, I., Rice, S. A., Ed.; John Wiley & Sons: New York, 1996; Vol. XCIII, p 219.
(22) Widmark, P.-O.; Malmqvist, P.-Å.; Roos, B. O. *Theor. Chim. Acta* **1990**, *77*, 291.
(23) Roos, B. O. The complete active space self-consistent field method and its applications in electronic structure calculations. In *Advances in Chemical Physics; Ab Initio Methods in Quantum Chemistry - II*; Lawley, K. P., Ed.; John Wiley & Sons Ltd.: Chichester, England, 1987. Chapter 69, p 399.
(24) Roos, B. O.; Andersson, K. *Chem. Phys. Lett.* **1995**, *245*, 215.
(25) Roos, B. O.; Andersson, K.; Fülscher, M. P.; Serrano-Andrés, L.; Pierloot, K.; Merchán, M.; Molina, V. *J. Mol. Struct. (THEOCHEM)* **1996**, *388*, 257.
(26) Malmqvist, P. Å.; Roos, B. O. *Chem. Phys. Lett.* **1989**, *155*, 189.
(27) Andersson, K.; Fülscher, M. P.; Karlström, G.; Lindh, R.; Malmqvist, P.-Å.; Olsen, J.; Roos, B. O.; Sadlej, A. J.; Blomberg, M. R. A.; Siegbahn, P. E. M.; Kellö, V.; Noga, J.; Urban, M.; Widmark, P.-O. *MOLCAS Version 3*; Department of Theoretical Chemistry, Chemical Centre, University of Lund, P.O.B. 124, S-221 00 Lund, Sweden, Lund, 1994.
(28) Xing, X.; Gedanken, A.; Sheybani, A.-H.; McDiarmid, R. *J. Phys. Chem.* **1994**, *98*, 8302.
(29) Demeo, D. A. Vacuum Ultraviolet and Photoelectron Studies of Olefins. Ph.D. Thesis, University of California at Los Angeles, 1969.
(30) Stidham, H. D. *Spectrochim. Acta* **1965**, *21*, 23.
(31) Kibel, M. H.; Livett, M. K.; Nyberg, G. L. *J. Electron Spectrosc. Relat. Phenom.* **1978**, *14*, 155.
(32) Bischof, V. P.; Hashmall, H. A.; Heilbronner, E.; Hornung, V. *Helv. Chim. Acta* **1969**, *52*, 1745.
(33) Doering, J. P. Unpublished results.
(34) Bischof, V. P.; Heilbronner, E. *Helv. Chim. Acta* **1970**, *53*, 1677.
(35) DiLauro, C.; Neto, N.; Califano, S. *J. Mol. Struct.* **1969**, *3*, 210.
(36) Carreira, L. A.; Carter, R. O.; Durig, J. R. *J. Chem. Phys.* **1973**, *59*, 812.
(37) Dallinga, G.; Toneman, L. H. *J. Mol. Struct.* **1967**, *1*, 117.
(38) Oberhammer, H.; Bauer, S. H. *J. Am. Chem. Soc.* **1969**, *91*, 10.
(39) Saebø, S.; Boggs, J. E. *J. Mol. Struct.* **1981**, *73*, 137.
(40) Sabljić, A.; McDiarmid, R.; Gedanken, A. *J. Phys. Chem.* **1992**, *96*, 2442.
(41) Sowers, B. L.; Arakawa, E. T.; Birkhoff, R. D. *J. Chem. Phys.* **1971**, *54*, 2319.
(42) Minnaard, N. G.; Havinga, E. *Recl. Trav. Chim. Pays-Bas* **1973**, *92*, 1179.
(43) Traetteberg, M. *Acta Chem. Scand.* **1968**, *22*, 2305.